Plasmonic Nanometric Optical Tweezers in an Asymmetric Space of Gold Nanostructured Substrates

Kodai Hirano[1], Hisashi Shimizu[1], Taira Enami[1], Mitsuhiro Terakawa[1], Minoru Obara[1,*], Nikolay N. Nedyalkov[2] and Petar A. Atanasov[2]

[1]*School of Integrated Design Engineering, Keio University, 3-14-1, Hiyoshi, Kohoku-ku, Yokohama-shi, 223-8522, Japan*

[2]*Institute of Electronics, Bulgarian Academy of Sciences, Tzarigradsko Shousse 72, Sofia 1784, Bulgaria*

Abstract: We present a plasmonic near-field tweezers in water with gold nanosphere pairs on various substrates. An enhanced near field localized in the nanometric gap space pumped with 800 nm femtosecond laser is to trap and kill small viruses. The maximal optical trapping force obtained is larger than 20 pN at an incident optical peak intensity of 1 mW/μm^2. We also propose a new system consisting of a gold nanosphere and a gold nanoridge. In this system, the enhanced near field stems mainly from the image charge effect, exhibiting an optical trapping in an asymmetric space. The calculated trapping force is equivalent to the system of gold nanosphere pairs. The trapped viruses may easily be inactivated using a unfocused 800 nm femtosecond laser.

Keywords: Plasmonic optical tweezers, near field optics, optical trapping, plasmonic dialysis of viruses ex vivo, femtosecond laser.

1. INTRODUCTION

Nanotechnology has developed rapidly, and the importance of manipulating nanoscale objects has been growing. Optical tweezers (trapping) is a state of the art technology. *Far-field* optical tweezers were reported by Ashkin *et al.* in 1986 [1]. Since then, optical tweezers have been studied extensively and have used in laboratory for the manipulation of micrometer-scale objects mainly in the field of biology and chemistry [2]. In addition to the Gaussian profile laser beam for trapping, many laser beam profiles have been used for optical trapping: rotational alignment of rod-like particles along the Bessel beam [2], optical trapping of atoms by using a doughnut beam [3], and optical trapping with holographic optical tweezers [4] were reported. Together with optical trapping performances, their applications were also reported: a subwavelength nanopatterning was done by the trapped microsphere as an objective lens [5] and two-photon luminescence from a trapped microsphere excited by femtosecond (fs) laser was observed [6].

Conventional optical trapping by using far-field optics can manipulate dielectric particles with several and tens of micrometers diameter. However, for nanoparticles, trapping force becomes very weak, and the Brownian motion becomes equivalent to the trapping force. The trapping volume of far-field optical tweezers cannot become smaller than a half optical wavelength due to the diffraction limit. Therefore, a *near-field* trapping using a surface plasmon-enhanced optical field is attractive for nanoparticle trapping [8]. Plasmonic 2D size-selective near-field trapping of micrometer-sized dielectric beads using 3.5-μm-diameter gold pillars was demonstrated [9]. This system requires no objective lens for laser focusing, and can trap multiple objects in multiple trapped areas by an unfocused single 785-nm laser beam. 3.5-μm particles were trapped 21 min after the laser irradiation. Plasmonically coupled pairs of gold nanodots have been also used for plasmonic optical trapping. Arrays of gold pairs exhibited a significant increase in trapping efficiency [10]. If the particles are aligned, higher optical field enhancement is generated between the particles due to the plasmon coupling [11]. The space for optical trapping is localized in the gap which is below the diffraction limit. The Brownian motion of a trapped nanoparticle is quenched more strongly by an order of magnitude than conventional optical tweezers, due to the enhanced optical near-field.

The nanometer and micrometer-scale structured substrates for near field optical trapping were fabricated mainly by using electron beam lithography. In addition, nanoimprint lithography [12] and nanolithography based on an atom pinhole camera [13] were reported. In addition, sophisticated self-assembling technology [14], nanosphere lithography [15-17], laser induced transfer (LIT) [18, 19], and others [20-22] were also proposed. These techniques are

*Address correspondence to this author at the School of Integrated Design Engineering, Keio University, 3-14-1, Hiyoshi, Kohoku-ku, Yokohama-shi, 223-8522, Japan; Tel: 81-45-566-1737; Fax: 81-45-566-1529;
E-mail: obara@obara.elec.keio.ac.jp

E-ISSN: 2311-8792

promising for high throughput fabrication of plasmonic nanostructured substrates.

In the meantime, gold nanoparticle pairs by simple technology are widely-used structures giving a high optical field enhancement factor in a nano-gap space. The spectral shift of plasmon resonance [23, 24], dependence of inter-particle distance [23, 24], and performance in heterodimer system [25, 26] were studied in detail. In these fields, many studies were focused on surface enhanced Raman spectroscopy (SERS), where the inter-particle distance of gold nanoparticle pairs is only a few nanometers [11, 25, 27].

In this paper, we present a plasmonic near-field tweezers in water with gold nanosphere pairs on various substrates of SiO_2, Si, and gold. The effect of substrate on the enhancement of near field of gold sphere between the substrate and the gold sphere was investigated primarily for nanocrater ablation processing: The near-field properties are studied for the case of a single isolated particle and 2D nanoparticle array [28, 29]. However, the effect of the substrate on the near field in the gap between the two gold particle pairs has not been made clear. An enhanced near field localized in the gap space between the two gold nanospheres pumped with 800 nm laser is used for near-field optical trapping, aiming at trapping and killing small viruses. The dependence of the enhanced plasmonic near field distribution on the substrate material is evaluated. In addition, we propose a new simple nanostructured trapping system consisting of a gold nanosphere and a gold nanoridge. The proposed structures exhibit a strong optical trapping force in an asymmetric space. The trapping force calculated is enough to trap nanometer scale viruses. The trapped viruses may be inactivated with an 800 nm fs laser pulse. Although plasmonic sensing of viruses was proposed [30, 31], the viruses trapped in a 3D nanospace with a unfocused 800 nm laser may be optically killed in the new system. The proposed system may potentially be used for *plasmonic dialysis* of viruses *ex vivo* in the blood flow of patients suffering from sepsis and/or an infectious disease like kidney dialysis. The water is optically quite transparent at 800 nm of fs laser. The *average* optical intensity of the fs laser is as low as 4 W/cm^2. This system is operating in water environment, which has a large heat capacity. Therefore, the thermal effect may be negligible in this scheme. The merit of using not cw laser but fs laser is to give trapping force *digitally* by the laser pulse number. Commercially available 80 MHz to 100 MHz-repetition-rate fs laser of 1 W average output without chirped pulse amplification (CPA) can easily be used to trap viruses in an enhanced plasmonic potential and simultaneously the trapped viruses may be deactivated by the enhanced pulsed optical field, while by reducing the intensity of fs laser pulses we can make non-destructive trapping of single viruses, being interesting to immobilize them and inspect them *via* multi-photon excitation. The average optical intensity of the unfocused fs laser is quite low and the thermal effect may be negligible in this scheme.

2. SIMULATION PROCEDURE

We first simulate near-field trapping characteristics in water by using gold nanosphere (NS) pairs on various substrate materials of SiO_2, Si, and Au. Figure **1** shows a schematic of size-selective near-field optical trapping to inactivate the trapped viruses by using 800 fs laser. An enhanced near field localized in the gap space between the two gold NSs pumped with 800 nm fs laser can be used for near-field optical trapping. The dependence of the enhanced optical near-field distribution on the substrate material was calculated using a 3D Finite-Difference Time-Domain (FDTD) method. The FDTD method gives good agreement with the experiments for the calculation of the enhanced optical field distribution of near-field light [32, 33].

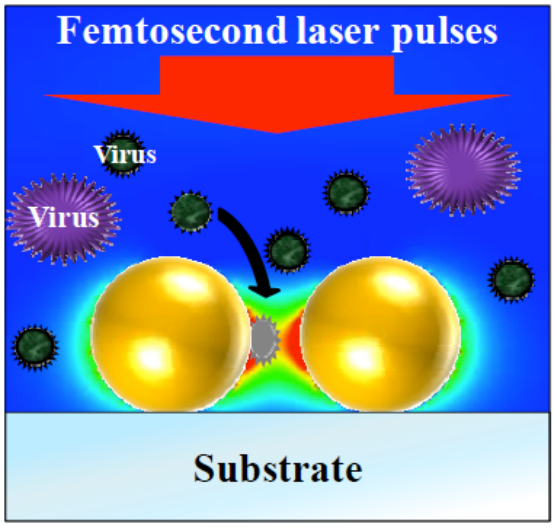

Figure 1: Schematic of concept for size-selective optical trapping and killing of viruses by using a 800 nm fs laser and gold NP pair.

Figure **2** shows a schematic of the simulation model. The model consists of a pair of gold NPs (diameter: *d*, gap distance: *g*) placed on a substrate in water (refractive index *n* = 1.329 at 800 nm). A *y*-polarized plane wave source of 800 nm wave length is set 1.2 μm above the substrate. Water shows little

optical absorption in a 800 nm region of the spectrum. Therefore, a 800 nm fs laser is suitable for bio-photonics applications. The minimum cell size is set to be 2.5×2.5×2.5 nm^3. The used boundary condition of ± *x* and ± *y* is periodic, and that of ± *z* is the Mur (absorbing) boundary condition. The simulation time is long enough to become a steady state (40 fs approximately after the start of laser irradiation). We defined enhancement factor $|E|^2/|E_0|^2$ as enhanced optical intensity at the steady state. The incident optical *E* field is set at 1 V/m.

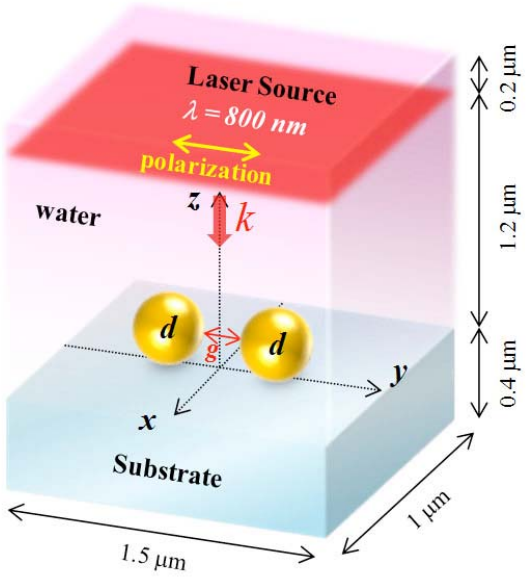

Figure 2: Schematic of the simulation model for gold NS pair.

3. SIMULATION RESULTS AND DISCUSSION

3.1. Dependence of Maximal Enhancement Factor in a Gap between Gold NS Pairs on Inter-Particle Distance

First, we calculated the optical field enhancement distribution around a pair of gold NSs (*d* = 200 nm) for gap distances of 5, 10, 20, 50, 100, 200, and 300 nm. The substrate material is a SiO_2 (n_{sub} = 1.538) substrate. Figure **3** shows the gap distance dependence of maximal enhancement factor. In this logarithmic graph, the dashed line shows a maximal enhancement factor obtained with a single gold NS (the inter-particle distance is infinite). The results indicate that the maximal enhancement factor decreases with increasing gap distance *g*. In the case of *g* > 100 nm, the maximal enhancement factor for the gold NPs is approaching that of a single gold NS. Then, we focus on a pair of gold NPs with gap distance of *g* = 50 nm, as shown by the red dotted line in Figure **3**, because it still exhibits a sufficiently high enhancement factor. Relatively small viruses such as yellow fever virus, norovirus, hepatitis B or C virus, etc. are smaller than 50 nm in dimension.

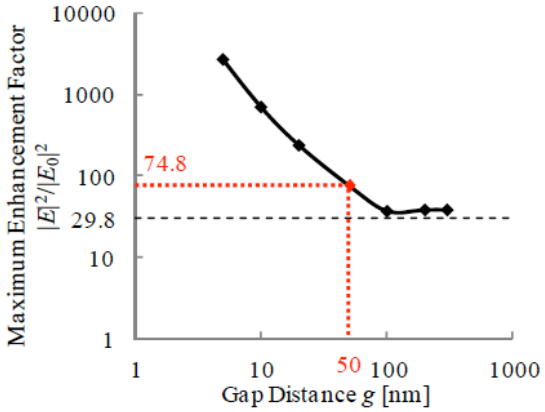

Figure 3: Dependence of the maximal enhancement factor on the gap distance. The diameter of gold NS is kept constant at *d* = 200 nm. The substrate material is SiO_2. A black dashed line shows the maximal enhancement factor achieved with a single gold NP on SiO_2.

3.2. Dependence of Enhancement Factor on NS Diameter and Substrate

We investigate the dependence of the field enhancement factor on the gold NS diameter at a gap distance of 50 nm. The enhancement factor distribution was calculated for diameter *d* ranging from 100 nm to 200 nm. The substrate materials are SiO_2, Si (n_{sub} = 3.68 + 0.00522*i*), and Au (n_{Au} = 0.188 + 5.39*i*). The optical properties (dielectric function) of the materials used in the calculations at 800 nm are taken from Ref. [34]. Figure **4** shows plots of the enhancement factor at the center of a gap (*x* = 0, *y* = 0, *z* = *d*/2) as a function of the diameter. The optimal diameter *d* for exhibiting a high enhancement factor was dependent upon the substrate material. The gold substrate exhibited the largest field enhancement factor among them.

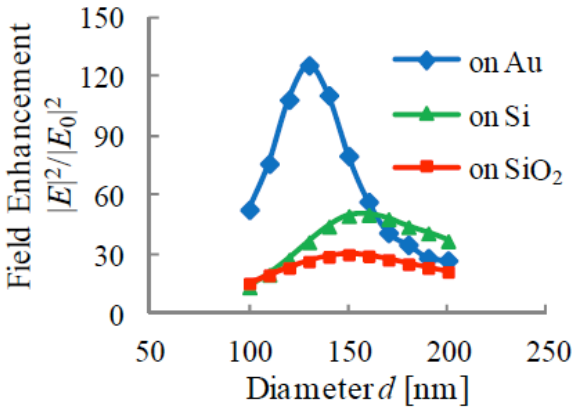

Figure 4: Dependence of the enhancement factor on the diameter at the gap center for the three different substrate materials, SiO_2, Si, and Au. The gap distance is constant at *g* = 50 nm.

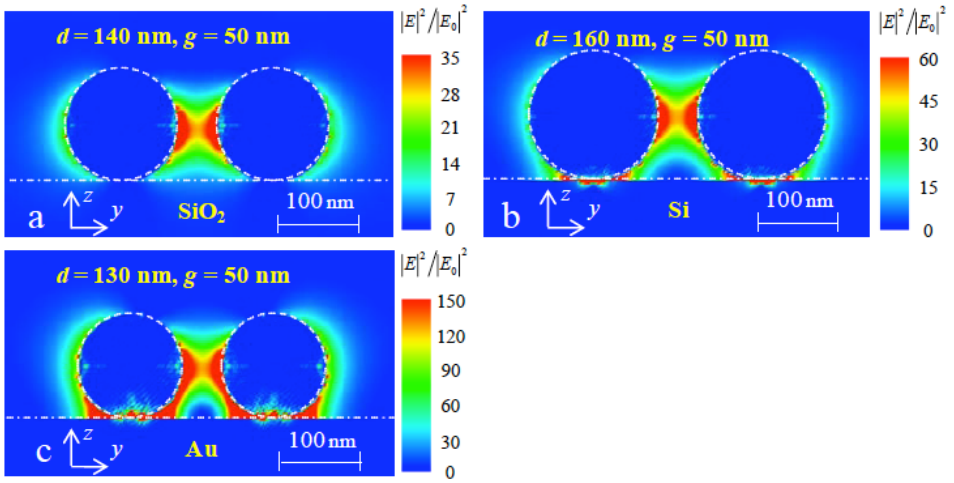

Figure 5: Enhanced field intensity distributions at the gap center for the three different substrate materials, SiO_2, Si, and Au. The gap distance is kept constant at g = 50 nm, while respective optimal diameter is different. Note that each intensity scale is different.

Figure **5** shows the enhancement factor distributions for the three substrates. Each inter-particle distance giving respective highest factor is used based on the data shown in Figure **4**. Enhanced field zones also appear under the gold NSs for Si and Au substrates, which do not appear in the case of SiO_2 substrate. The enhanced zone at the contact point is due to the contribution of the image charge in the high-refractive-index and metal substrates [29, 32, 33].

The amount of image charge q' inside dielectric material is written as the following equation

$$q' = -\frac{\varepsilon_{sub} - \varepsilon_m}{\varepsilon_{sub} + \varepsilon_m} q, \quad (1)$$

where q is the amount of the charge, ε_m is permittivity of the surrounding medium, and ε_{sub} is that of the substrate. If the Si substrate has a higher permittivity, the plasmon coupling between NSs and the Si substrate becomes stronger. However, an optical intensity is not enhanced at the contact point between gold NS and the SiO_2 substrate, because the difference of permittivity between SiO_2 and water is little.

Figure **6** shows the charge density distribution. This charge density distribution determines the optical field distribution. Figure **6a** shows a low density charge distribution for the SiO_2 substrate, while Figure **6b** shows the higher charge density distribution for the Si substrate. The amount of image charge inside an ideal conductor metal is written by the following equation

$$q' = -q. \quad (2)$$

As for the Au substrate, the charge density is significantly higher than either SiO_2 or Si (Figure **6c**). As the plasmon coupling between NPs and the

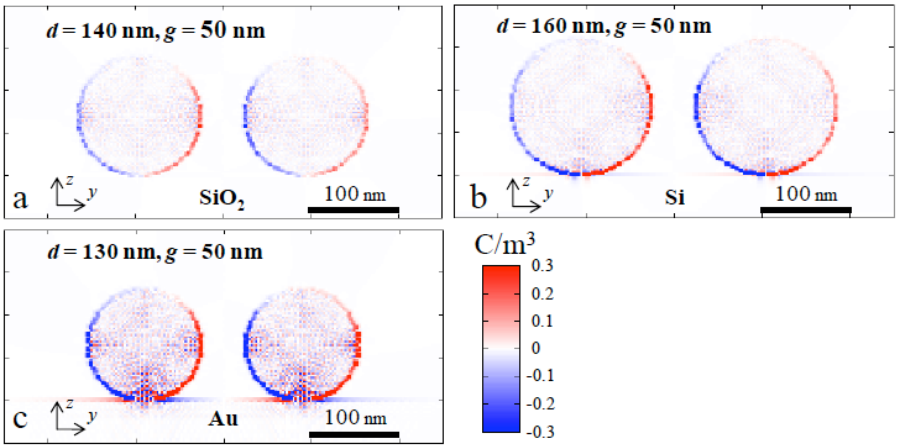

Figure 6: Charge density distributions around gold NSs derived from the enhanced field intensity distribution shown in Figure **5**. The substrate materials in **a**, **b**, and **c** are SiO_2, Si, and Au, respectively. The steady state charge density at 39.365 fs after the fs irradiation is shown.

substrate becomes stronger, an enhancement factor is also increased in the gap of gold NP pairs.

M13 bacteriophages are inactivated at a threshold intensity of about 60 MW cm^{-2}, while Tobacco mosaic virus (TMV) is inactivated at a threshold intensity of about 250 MW cm^{-2} [35]. Therefore, these data provide strong support that target viruses have an inactivation threshold of the order of a few hundred MW cm^{-2} or lower when illuminated with a near-IR 80 fs laser. The HIV samples are irradiated with 776 nm, 500 fs pulse [36]. It is found that HIV *in vitro* remains infectious when irradiated with laser intensities of lower than about 500 MW cm^{-2}. However, as the laser intensity exceeds 1.1 GW cm^{-2}, HIV loses its infectivity.

In the case of Au substrate, we obtained a 150-fold increase in the optical intensity in the gap in relation to the incident intensity. Therefore, this highly enhanced intensity can inactivate such trapped viruses with 800 nm fs laser at incident intensities of tens of MW cm^{-2}, which are easily obtainable with commercially-available fs laser oscillators without CPA.

3.3. Optical Trapping Force Distribution in a Gap Space

The optical force for trapping a polystyrene sphere (PSS) of 50 nm diameter as a model sample of virus is calculated from the result shown in Figure **5c**. The PSS is widely used for the evaluation of optical trapping force [1, 4, 5, 9, 10]. If the trapped particle's diameter is smaller than the incident laser wavelength, optical force F is written as the following equation

$$F = -\frac{n_m}{2}\alpha \nabla E^2, \tag{3}$$

where n_m is the refractive index of the surrounding medium and α is the polarizability of the trapped object. The effective particle polarizability α is expressed by

$$\alpha = 4\pi r^3 \frac{\varepsilon_p - \varepsilon_m}{\varepsilon_p + 2\varepsilon_m}, \tag{4}$$

where r is radius of the trapped particle, ε_m is permittivity of the surrounding medium, and ε_p is permittivity of the trapped particle.

The obtained optical force is shown in Figure **7**. The incident laser intensity is assumed as 1 mW/μm^2. At this laser intensity, a maximal trapping force is larger than 20 pN, as shown in Figure **7c**. As the high trapping force is generated only in the gap, larger objects than the gap size cannot be trapped. The trapping stiffness reported in a plasmonic near-field trapping is 0.013 pN/nm/W [10] for trapping of a PSS of 200 nm diameter (λ = 1064 nm) and 6.6 pN/nm/W [37] for trapping of a PSS of 50 nm diameter (λ = 1064 nm). The values of trapping stiffness are not directly compared, because the experimental parameters of the

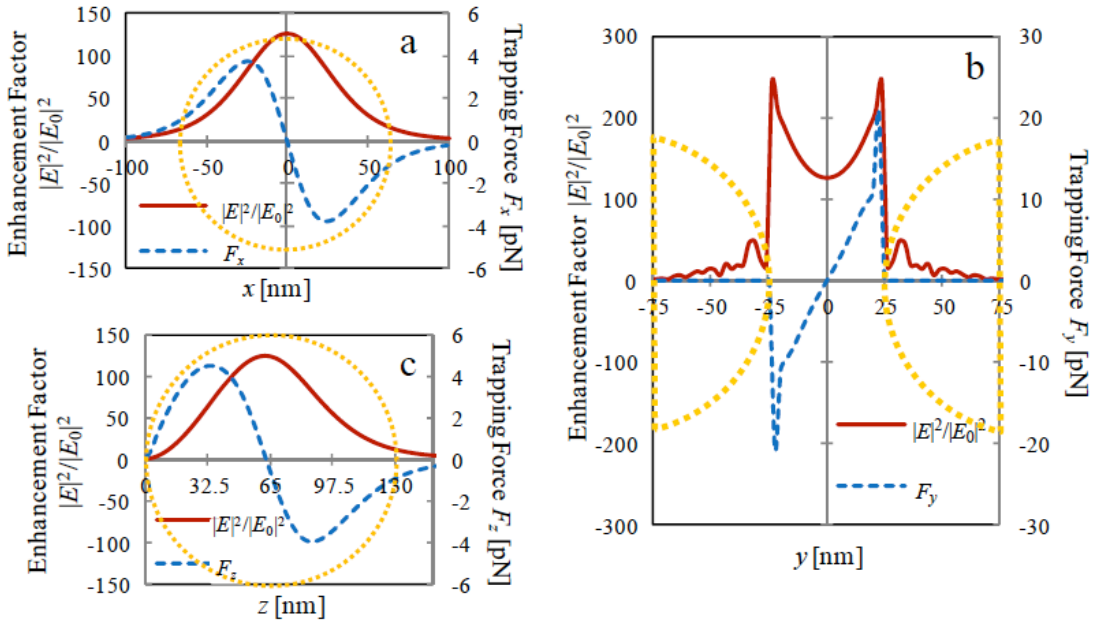

Figure 7: Optical force distribution for a 50-nm-diameter PSS in the gap space. The gold NPs are on the Au substrate (see Figure **5c**). **a, b, c** show the optical force of x direction (y = 0, z = d/2 = 65 nm), y direction (x = 0, z = d/2 = 65 nm), and z direction (x = 0, y = 0), respectively. The incident laser intensity is assumed as 1 mW/μm^2 (0.1 MW/cm^2). Yellow dotted circles indicate the lineation of gold NP.

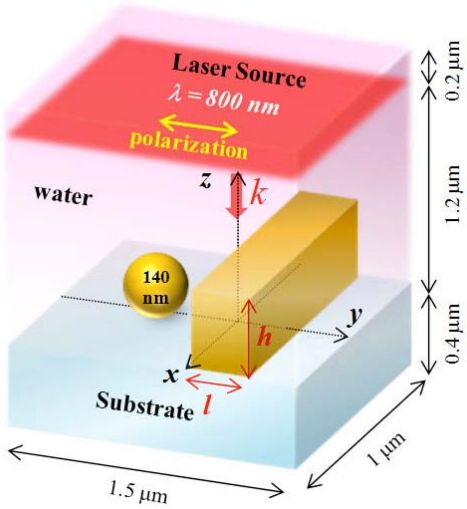

Figure 8: Schematic of the simulation model for a gold NP and a gold NR.

used substrate material and the incident wavelength are different. In the present scheme, a similar value of trapping stiffness to the previous reports was achieved.

The proposed system may potentially be used for plasmonic dialysis of viruses ex vivo in the blood flow of patients suffering from sepsis and/or an infectious disease like kidney dialysis. The water is optically quite transparent at 800 nm of fs laser. Commercially available 80 MHz to 100 MHz-repetition-rate fs laser of 1 W average power without chirped pulse amplification (CPA) can trap viruses in an enhanced plasmonic potential and simultaneously the trapped viruses may be deactivated by the enhanced pulsed optical field. With low intensity fs laser pulses we can make non-destructive trapping of single viruses, that is interesting to immobilize them and inspect them *via* such as multi-photon excitation.

The water is optically quite transparent at 800 nm of fs laser. The average optical intensity of the fs laser is quite low. This system is operating in water environment, which has a large heat capacity. Therefore, the thermal effect may be negligible in this scheme.

3.4. Optical Trapping Using a Gold NS and a Gold Nanoridge

We also investigate a new nanostructure system, in which the one gold NS in pairs is replaced with a gold nanoridge (NR, height *h*, thickness *l*). This concept comes from the mirror image structure in laser resonators. In far-field optics, the confocal Fabry-Perot type resonator is identical to the semi-confocal one with a half reflectors separation, in which the resonator mode volume is asymmetric. In near field optics, this nano-structure system would be identical to the NS pairs from the electromagnetics viewpoint. A schematic of the 3D FDTD calculation model for this new nanostructure system is shown in Figure **8**. The gap distance *g* is 50 nm in order to reserve a space for trapping yellow fever virus, norovirus, etc. The merit of this system is to trap a specimen *three dimensionally*, while the gold slot geometry with the two ridges is to trap a specimen only *one dimensionally*.

The field intensity enhancement factor distribution for different thickness *l* is shown in Figure **9**. In this case, the substrate material is SiO_2. If a gold NR of *l* = 50 nm and *h* = 140 nm is used, a high enhancement factor is obtained in a gap space of 50 nm separation, being equivalent to the system of gold NP pairs described above. The enhancement factor distribution shown in Figure **9b** is consistent with that in Figure **9a**, mainly due to the image charge effect in the gold NR.

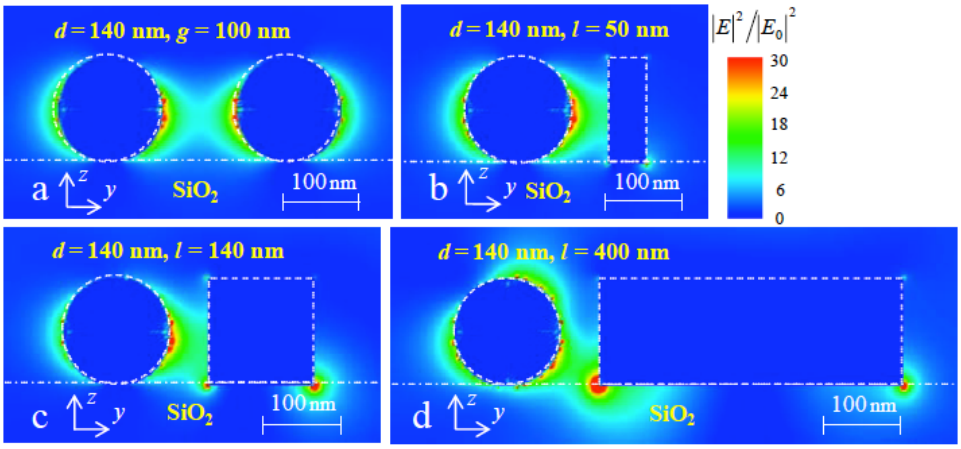

Figure 9: Enhanced field intensity distributions factor around a gold NP and a gold NR on the SiO_2 substrate. **a** shows the distribution of gold NP pairs with gap distance of 100 nm. Thickness *l* of a gold NR in **b**, **c**, and **d** is 50 nm, 140 nm, and 400 nm, respectively. The height of the gold NR is kept constant at *h* = 140 nm. The gap length for **b**, **c** and **d** is 50 nm.

Figure **10** shows the charge density distributions calculated from the enhancement field distribution shown in Figure **9**. This charge density distribution determines the optical field distribution. Calculating the Poynting vector (data not shown), it can be seen that the incident optical energy is efficiently delivered into the gap space. This structure well behaves like the gold NP pairs system. As the thickness *l* of the gold NR increases, the optical enhancement factor at the bottom edge of the gold NR is increased. Because the plasmon coupling between the gold NS and the bottom of gold NR becomes stronger, the high intensity zone moves toward the substrate. Conversely, by using a gold substrate and a high gold NR (*h* = 200 nm), the plasmon coupling between the gold NS and the edge of the gold NR is decreased, and a high enhancement factor is achieved in the gap of 50 nm, even if the gold NR is 400 nm thick, as shown in Figure **11**. The optical force for trapping is shown in Figure **12** in this system is found comparable to that of gold NP pairs shown in Figure **7**.

4. CONCLUSION

In this paper, we proposed and revisited a size-selective asymmetric near-field optical trapping system using gold NS pairs. The dependence of the field intensity enhancement factor distribution on the substrate material was presented. By using a 130-nm-diameter gold NS pairs on the Au substrate, a high enhancement factor (about a 150-fold increase of the incident 800 nm laser intensity) is obtainable even for the wide gap distance (g = 50 nm). By using this structure, a maximal optical trapping force is larger than 20 pN for a 50-nm-diameter PSS at an incident optical *peak* intensity of 1 mW/μm^2 (0.1 MW/cm^2). The average optical intensity of the fs laser is quite low and the thermal effect may be negligible in this scheme. This system is operating in water environment, which has a large heat capacity.

We also proposed a new structure system consisting of a gold NS and a gold NR on the Au substrate. It is shown that the asymmetric gap space gives a high enhancement factor. From the

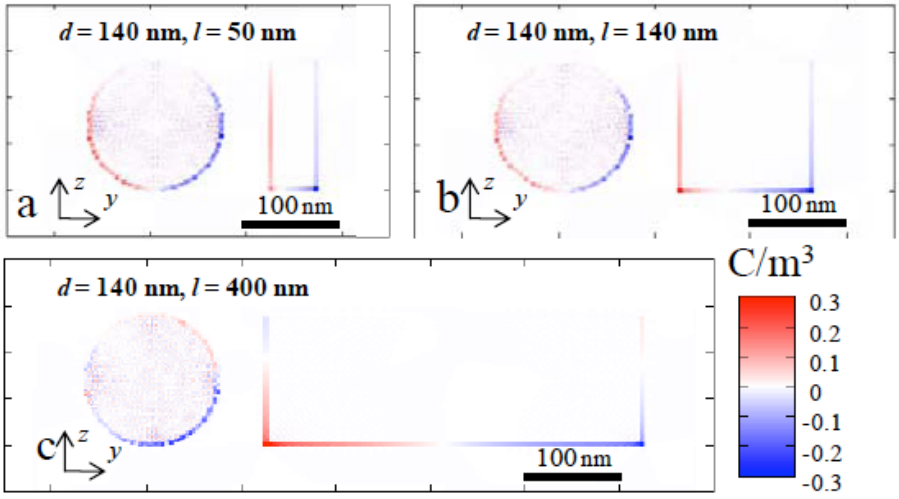

Figure 10: Charge density distributions calculated from the field intensity distribution in Figure **9**. Thickness *l* of gold NR in (**a**), (**b**), and (**c**) is 50 nm, 140 nm, and 400 nm, respectively.

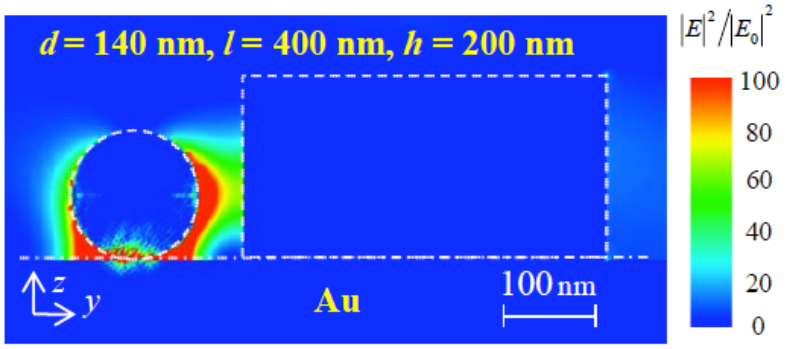

Figure 11: Enhanced field intensity distribution around a gold NP and a thick gold NR on the Au substrate (diameter *d* = 140 nm, thickness *l* = 400 nm, and height *h* = 200 nm).

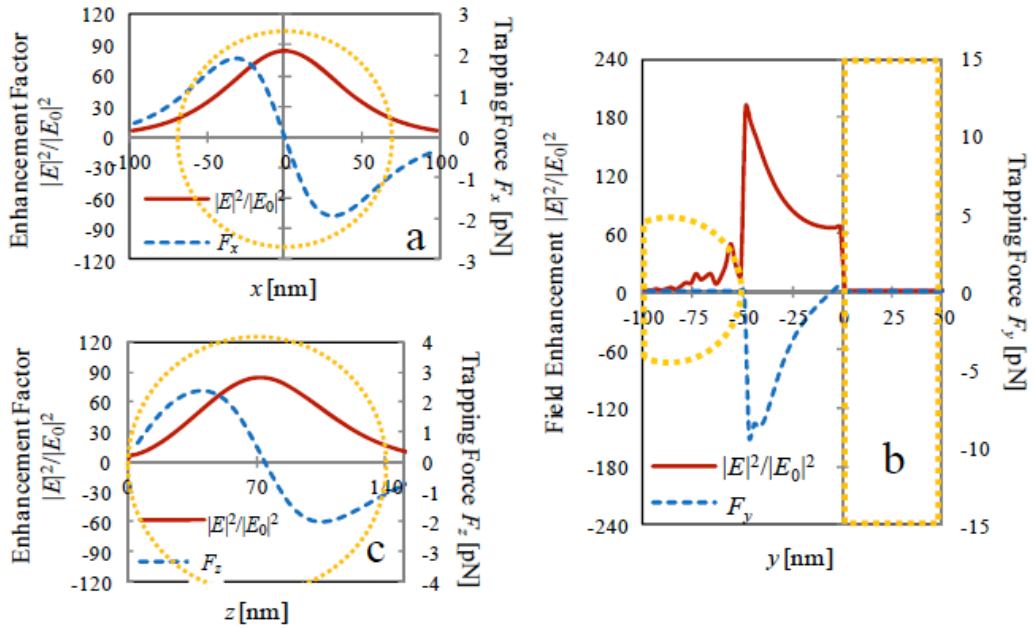

Figure 12: Optical force for a 50-nm-diameter PS particle in the gap space (see Figure **11**). **a, b, c** show that of *x* direction (*y* = -*g*/2 = -25 nm, *z* = *d*/2 = 70 nm), *y* direction (*x* = 0, *z* = *d*/2 = 70 nm), and *z* direction (*x* = 0, *y* = -*g*/2 = -25), respectively. The incident laser intensity is assumed as 1 mW/μm^2 (0.1 MW/cm^2). Yellow dotted circles indicate lineation of gold NP.

electromagnetics viewpoint, this system would be identical to the gold NS pairs geometry.

A plasmonic near-field trapping with these nanostructures has the advantage over conventional far-field optical tweezers, because the proposed nanostructures enable optical size-selective trapping of smaller samples than the gap space. This system has a potential to trap and inactivate viruses with one 800 nm fs laser pulse irradiation. Of course, we can optimize the trapping system to give highest trapping force for respective size of specimen in plasmonic near-field optics. The proposed system may potentially be used for *plasmonic dialysis* of viruses *ex vivo* in the blood flow of patients suffering from sepsis and/or an infectious disease like kidney dialysis.

ACKNOWLEDGEMENTS

This study was supported in part by a Grand-in-Aid for Scientific Research (B-23360161) from MEXT Japan.

REFERENCES

[1] Ashkin A, Driedzic JM, Bjorkholm JE, Chu S. Observation of a single-beam gradient force optical trap for dielectric particles. Opt Lett 1986; 11(5): 288-90. http://dx.doi.org/10.1364/OL.11.000288

[2] Arlt J, Garces-Chavez V, Sibbett W, Dholakia K. Optical micromanipulation using a Bessel light beam. Optics Comm 2001; 197: 239-45. http://dx.doi.org/10.1016/S0030-4018(01)01479-1

[3] Kuga T, Trii Y, Shiokawa N, Hirano T. Novel optical trap of atoms with a doughnut beam. Phys Rev Lett 1997; 78(25): 4713-16. http://dx.doi.org/10.1103/PhysRevLett.78.4713

[4] Curtis JE, Koss BA, Grier DG. Dynamic holographic optical tweezers. Optics Comm 2002; 207(1-6): 169-75. http://dx.doi.org/10.1016/S0030-4018(02)01524-9

[5] Mcleod E, Arnold CB. Subwavelength direct-write nanopatterning using optically trapped microspheres. Nature Nanotech 2008; 3: 413-17. http://dx.doi.org/10.1038/nnano.2008.150

[6] Agate B, Brown CTA, Sibbett W, Dholakia K. Femtosecond optical tweezers for in-situ control of two-photon fluorescence. Opt Express 2004; 12(13): 3011-17. http://dx.doi.org/10.1364/OPEX.12.003011

[7] Savitski VG, Metzger NK, Calvez S, Burs D, Sibbett W, Brown CTA. Optical trapping with “on-demand” two-photon luminescence using Cr:LiSAF laser with optically addressed saturable Bragg reflector. Opt Express 2012; 20(7): 7066-70. http://dx.doi.org/10.1364/OE.20.007066

[8] Juan ML, Righini M, Quidant R. Plasmon nano-optical tweezers. Nat Photonics 2011; 5(6): 349-56. http://dx.doi.org/10.1038/nphoton.2011.56

[9] Righini M, Zelenina AS, Girard C, Quidant R. Parallel and selective trapping in a patterned plasmonic landscape. Nat Phys 2007; 3: 477-80. http://dx.doi.org/10.1038/nphys624

[10] Grigorenko AN, Roberts NW, Dickinson MR, Zhang Y. Nanometric optical tweezers based on nanostructured substrates. Nat Photonics 2008; 2: 365-70. http://dx.doi.org/10.1038/nphoton.2008.78

[11] Xu H, Bjerneld EJ, Kall M, Borjesson L. Spectroscopy of single hemoglobin molecules by Surface Enhanced Raman Scattering. Phys Rev Lett 1999; 83(21): 4357-60. http://dx.doi.org/10.1103/PhysRevLett.83.4357

[12] Boltasseva A. Plasmonic components fabrication *via* nanoimprint. J Opt A: Pure Appl Opt 2009; 11(11): 114001-11. http://dx.doi.org/10.1088/1464-4258/11/11/114001

[13] Melentiev PN, Zablotskiy AV, Lapashin DA, Sheeshin EP, Baturin AS, Balykin VI. Nanolithography based on an atom pinhole camera. Nanotechnology 2009; 20(23): 235301-7. http://dx.doi.org/10.1088/0957-4484/20/23/235301

[14] Lee W, Lee SY, Briber RM, Rabin O. Self-assembled SERS substrates with tunable surface plasmon resonances. Adv Funct Mater 2011; 21(18): 3424-29. http://dx.doi.org/10.1002/adfm.201101218

[15] Haynes CL, Duyne RPV. Nanosphere lithography: A versatile nanofabrication tool for studies of size-dependent nanoparticle optics. J Phys Chem B 2001; 105(24): 5599-11. http://dx.doi.org/10.1021/jp010657m

[16] Huang W, Qian W, El-Sayed MA. Photothermal reshaping of prismatic Au nanoparticles in periodic monolayer arrays by femtosecond laser pulses. J Appl Phys 2005; 98(11): 114301-8. http://dx.doi.org/10.1063/1.2132515

[17] Song KH, Lee HY. Fabrication of two-dimensional photonic crystals with Ge2Sb2Te5 nanohole arrays by nanosphere lithography. International J Modern Physics B 2009; 23(6-7): 1300-305. http://dx.doi.org/10.1142/S0217979209060853

[18] Kuznetsov AI, Kiyan R, Chichkov BN. Laser fabrication of 2D and 3D metal nanoparticle structures and arrays. Opt Express 2010; 18(20): 21198-203. http://dx.doi.org/10.1364/OE.18.021198

[19] Kuznetsov AI, Evlyukhin AB, Gonç alves MR, Reinhardt C, Koroleva A, Arnedillo ML, *et al*. Laser fabrication of large-scale nanoparticle arrays for sensing applications. ACS Nano 2011; 5(6): 4843-49. http://dx.doi.org/10.1021/nn2009112

[20] Hartling T, Alaverdyan Y, Hille A, Wenzel MT, Kall M, Eng LM. Optically controlled interparticle distance tuning and welding of single gold nanoparticle pairs by photochemical metal deposition. Opt Express 2008; 16(16): 12362-71. http://dx.doi.org/10.1364/OE.16.012362

[21] Alexander KD, Hampton MJ, Zhang S, Dhawan A, Xu H, Lopez R. A high-throughput method for controlled hot-spot fabrication in SERS-active gold nanoparticle dimer arrays. J Raman Spectrosc 2009; 40(12): 2171-75. http://dx.doi.org/10.1002/jrs.2392

[22] Yan B, Thubagere A, Premasiri WR, Ziegler LD, Negro LD, Reinhard BM. Engineered SERS substrates with multiscale signal enhancement: Nanoparticle cluster arrays. ACS Nano 2009; 3(5): 1190-202. http://dx.doi.org/10.1021/nn800836f

[23] Rechberger W, Hohenau A, Leitner A, Krenn JR, Lamprecht B, Aussenegg FR. Optical properties of two interacting gold nanoparticles. Opt Comm 2003; 220(1-3): 137-41. http://dx.doi.org/10.1016/S0030-4018(03)01357-9

[24] Yang SC, Kobori H, He CL, Lin MH, Chen HY, Li C, *et al*. Plasmon hybridization in individual gold nanocrystal dimers: Direct observation of bright and dark modes. Nano Lett 2010; 10(2): 632-37. http://dx.doi.org/10.1021/nl903693v

[25] Brown LV, Sobhani H, Lassiter JB, Nordlander P, Halas NJ. Heterodimers: Plasmonic properties of mismatched nanoparticle pairs. ACS Nano 2010; 4(2): 819-32. http://dx.doi.org/10.1021/nn9017312

[26] Slaughter LS, Wu Y, Willingham BA, Nordlander P, Link S. Effects of symmetry breaking and conductive contact on the plasmon coupling in gold nanorod dimers. ACS Nano 2010; 4(8): 4657-66. http://dx.doi.org/10.1021/nn1011144

[27] Du CL, Du CJ, You YM, He CJ, Luo J, Shi DN. Surface-Enhanced Raman Scattering from individual Au nanoparticles on Au films. Plasmonics 2012; 7: 475-78. http://dx.doi.org/10.1007/s11468-012-9331-y

[28] Nedyalkov N, Sakai T, Miyanishi T, Obara M. Near field properties in the vicinity of gold nanoparticles placed on various substrates for precise nanostructuring. J Physics D 2006; 39(23): 5037-42. http://dx.doi.org/10.1088/0022-3727/39/23/021

[29] Nedyalkov NN, Atanasov PA, Obara M. Near-field properties of a gold nanoparticle array on different substrates excited by a femtosecond laser. Nanotechnology 2007; 18(30): 305703-7. http://dx.doi.org/10.1088/0957-4484/18/30/305703

[30] Fan X, White IM, Shopova SI, Zhu H, Suter JD, Sun Y. Sensitive optical biosensors for unlabeled targets: A review. Anal Chem Acta 2008; 620: 8-26. http://dx.doi.org/10.1016/j.aca.2008.05.022

[31] Dantham VR, Holler S, Kolchenko V, Zan W, Arnold S. Taking whispering gallery-mode single virus detection and sizing to the limit. Appl Phys Lett 2012; 101(4): 043704-4. http://dx.doi.org/10.1063/1.4739473

[32] Terakawa M, Takeda S, Tanaka Y, Obara G, Miyanishi T, Sakai T, *et al*. Enhanced localized near field and scattered far field for surface nanophotonics applications. Progress in Quantum Electron 2012; 36(1): 194-71. http://dx.doi.org/10.1016/j.pquantelec.2012.03.006

[33] Miyanishi T, Sakai T, Nedyalkov NN, Obara M. Femtosecond-laser nanofabrication onto silicon surface with near-field localization generated by plasmon polaritons in gold nanoparticles with oblique irradiation. Appl Phys A 2009; 96(4): 843-50. http://dx.doi.org/10.1007/s00339-009-5313-0

[34] Palik ED. Handbook of Optical Constants of Solids. San Diego, CA: Academic Press 1998.

[35] Tsen KT, Tsen SWD, Sankey OF, Kiang JG. Selective inactivation of micro-organisms with near-infrared femtosecond laser pulses. J Phys: Condens Matter 2007; 19(47): 472201-7. http://dx.doi.org/10.1088/0953-8984/19/47/472201

[36] Tsen KT, Tsen SWD, Hung CF, Wu TC, Kiang JG. Selective inactivation of human immunodeficiency virus with subpicosecond near-infrared laser pulses. J Phys: Condens Matter 2008; 20(25): 252205-4. http://dx.doi.org/10.1088/0953-8984/20/25/252205

[37] Serey X, Mandal S, Erickson D, Comparison of silicon photonic crystal resonator designs for optical trapping of nanomaterials. Nanotechnology 2010; 21(30): 305202-8. http://dx.doi.org/10.1088/0957-4484/21/30/305202

Received on 27-03-2013 Accepted on 29-03-2013 Published on 22-08-2013

DOI: http://dx.doi.org/10.12974/2311-8792.2013.01.01.1